Gadolinium-Enhanced Magnetic Resonance Imaging of Atherosclerotic Plaques in Comparison with Histopathology: An In Vivo Study in Aorta of Rabbits

Byoung Wook Choi, Jin Hur, Hye-Jeong Lee, Young Jin Kim, Tae Hoon Kim, Kyu Ok Choe

Purpose : We sought to evaluate enhancement of plaque with gadolinium-based contrast agent by magnetic resonance imaging (MRI) in comparison with histopathology, namely lipid-rich and macrophage-rich components that were two representative characteristics of plaque vulnerability using atherosclerotic rabbit aorta in order to determine which histopathologic component is relevant to the enhancement.

Materials and Methods : New Zealand white rabbit (n = 4, weight 3.0 to 3.5 kg, all male) was used for animal model of atherosclerosis. Atherosclerotic aortic lesions were induced by high-cholesterol diet and double balloon injury. T1-weight axial images were acquired before and after gadolinium-based contrast agent using a 3-T MRI. MR images and the matched histopathological sections (n = 35) were divided into 4 quadrants or 3 (n = 130). Enhancement ratio (ER, ER = SIpost/SIpre) on MRI was calculated for each quadrant and compared with histopathology in regard to lipid-rich and macrophage-rich areas.

Results : Lipid-rich quadrants were 72 and fibrous quadrants were 58. The number of quadrants which had macrophage-rich areas was 105 and that of quadrants which did not have macrophage-rich areas was 25. ER was significantly higher in lipid-rich quadrants than in fibrous quadrants (mean ER 2.25 ± 0.41 vs. 2.72 ± 0.65, p = 0.013). ER poorly correlated with macrophage-rich areas when lipid-component was controlled (correlation coefficient -0.203, p = 0.236).

Conclusion : Lipid-rich plaques showed stronger enhancement than fibrous plaques using a standard gadolinium-based extracellular contrast agent. Macrophage infiltration did not correlate with degree of enhancement. Further study is warranted that account for optimal time of imaging after contrast injection using various plaque models from early to advanced stages and all possible parameters associated with contrast enhancement.

Index words : Atherosclerotic plaque
Plaque vulnerability
Contrast-enhanced magnetic resonance imaging
Lipid-rich plaque, Macrophage

Introduction

Conventional angiography has been a standard modality to diagnose degree of stenosis of coronary artery. However it does not provide any information with regard to plaque composition and inflammatory activity. Growing evidence suggests that the decisive factor determining plaque vulnerability is plaque composition rather than the degree of luminal narrowing (1–3). Vulnerable plaque has characteristic features of a large lipid core, a thin fibrous cap, and abundant macrophages and neovessels as an inflammatory activity (4). Magnetic resonance imaging (MRI) with high spatial resolution has shown great promise in the identification and quantification of atherosclerotic plaque components which are related to plaque vulnerability (5–12).

Contrast-enhanced MRI using gadolinium-based extracellular contrast agents offers morphological as well as functional assessment of atherosclerotic plaque formation (5–10). Contrast-enhanced MRI has been found useful for the characterization of fibrous plaque tissue in patients with advanced carotid artery stenosis (5, 6). Recent studies on human carotid atherosclerotic plaques have shown that several gadolinium uptake parameters correlated with the extent of macrophage burden (7). However, gadolinium-based contrast agents are not specific, and the underlying mechanisms leading to contrast enhancement within the atherosclerotic vessel wall are so far not fully elucidated.

With current MR technology, evaluation of atherosclerotic plaques in human coronary artery is limited. Rabbit aorta is well established atherosclerotic model for plaques in human coronary artery because the size of vessel is similar to that of human coronary artery and high cholesterol diet with double balloon injury technique to induce atherosclerosis in the aorta of rabbit has been proved to be efficient even though there is no concrete evidence that the characteristics or contrast-enhancement of plaques in rabbit aorta is the same as those of coronary artery or carotid artery.

In this study, we sought to evaluate enhancement of plaque with gadolinium-based contrast agent by MRI in comparison with histopathology, namely lipid-rich and macrophage-rich components that were two representative characteristics of plaque vulnerability using atherosclerotic rabbit aorta in order to determine which histopathologic component is relevant to the enhancement.

Materials and Methods

Animal Protocol

New Zealand white rabbit (n = 4, weight 3.0 to 3.5 kg, all male) was used for animal model of atherosclerosis. Atherosclerotic aortic lesions were induced by 4 months of a high-cholesterol diet (1% cholesterol and 5% coconut oil) and double aortic balloon denudation injury (at 1 week and 1 month after starting the high-cholesterol diet). Aortic injury was performed 3 times from the aortic arch to the iliac bifurcation with use of a 4F Fogarty embolectomy catheter introduced through the iliac artery. All procedures were performed under general anesthesia by intramuscular ketamine injection (30 mg/kg) and xylazine (10 mg/kg). The study protocol was approved by our Animal Care and Use Committee.

Magnetic Resonance Imaging

Under general anesthesia by intramuscular ketamine injection (20 mg/kg) and xylazine (5 mg/kg), the rabbits were imaged in the craniocaudal direction and in the supine position with a 3.0 Tesla (T) MRI unit (TrioTim, Siemens Medical Systems, Germany) using the body coil. Three orthogonal localizer images served to confirm an adequate position of the animal. Thereafter, sequential axial T1-weighted images with a 3-mm thickness of the aorta from the arch to the iliac bifurcation were obtained using a fast spin-echo sequence with an in-plane resolution of 0.43×0.43 mm. Two minutes after administration of 0.1mmol/kg of gadolinium-based contrast agent (Gadodiamide, OmniscanTM, 0.5 mmol/ml, GE Healthcare) via the ear vein, axial T1-weighted imaging was repeated with the same protocol as pre-contrast scan. Each T1-weighted imaging typically took 15 minutes. Fat suppression was applied in all imaging sequences. The typical parameters were as follows; TR/TE: 624/10 ms, field of view = 11×11 cm, matrix 256×256, echo train length = 5, signal averages = 2.
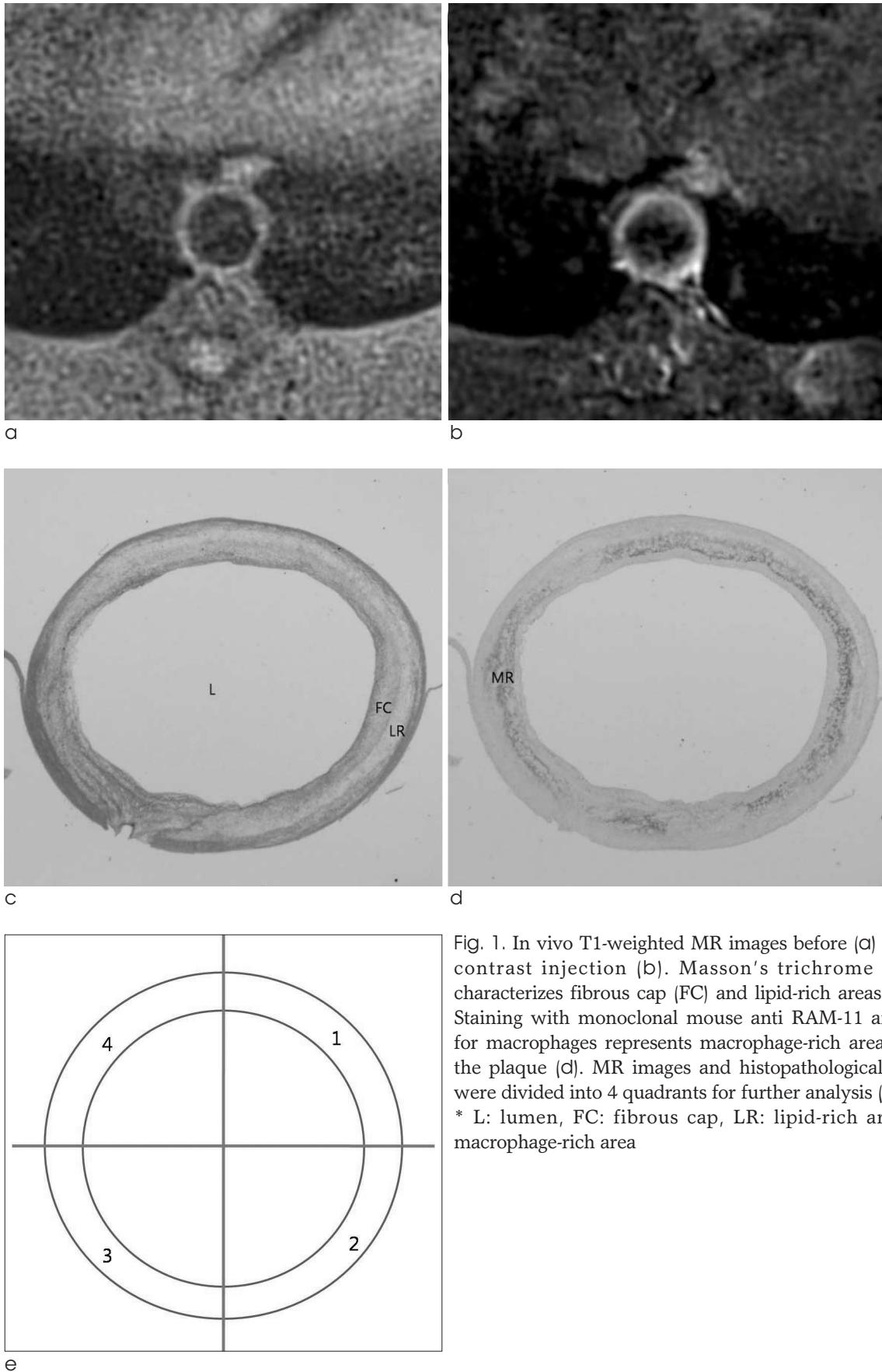
a

b

c

d

e

Fig. 1. In vivo T1-weighted MR images before (a) and after contrast injection (b). Masson's trichrome staining characterizes fibrous cap (FC) and lipid-rich areas (LR) (c). Staining with monoclonal mouse anti RAM-11 antibodies for macrophages represents macrophage-rich area (MR) in the plaque (d). MR images and histopathological sections were divided into 4 quadrants for further analysis (e).
* L: lumen, FC: fibrous cap, LR: lipid-rich area, MR: macrophage-rich area

Histopathology

Rabbits were euthanized within 48 hours after MRI by intravenous injection of 5 mL IV of 26% sodium pentobarbital after receiving heparin (1000 U/kg) to prevent postmortem thrombosis.

The aortas were excised after the perfusion-fixation using 4% phosphate-buffered paraformaldehyde (4% in PBS). Serial sections of the aorta were cut at 3-mm intervals to match the corresponding MR images. Specimens were embedded in paraffin, and sections 5 μm thick were cut for one per every 3 slices and stained with combined Masson's trichrome elastin stain. Additional sections were stained with monoclonal mouse anti RAM-11 antibodies for macrophages (Dako, CA, USA).

Image Analysis

The MR images were transferred to a dedicated workstation (Aquarius, Terrarecon Inc) for analysis. Wall and lumen signal intensities (SI) were determined with standard region-of-interest (ROI) measurements with magnification. One experienced radiologist who was dedicated to cardiovascular imaging drew all ROIs. Enhancement ratio (ER) of the SI was calculated as follows; ER = SIpost/SIpre, where SIpost is SI of the wall after contrast enhancement and SIpre is SI of the wall before contrast enhancement. An experienced radiologist performed all measurements.

The histopathologic sections were digitized from a camera attached to a light microscope then transferred to another computer. An independent pathologist blinded to the results of MRI performed the histopathology analysis.

MR images and the matched histopathological sections (n = 35) were divided into 3 or 4 quadrants (n = 130) (Fig. 1). ER was calculated for each quadrant of MR images and was thereafter classified as lipid-rich or fibrous plaque on the basis of histological sections. On histological analysis, if the percentage of lipid rich areas was over 50% of total plaque area, then it was considered as a lipid-rich plaque. Macrophage-rich areas were measured by manual drawing of ROI at the areas which were stained with monoclonal mouse anti RAM-11 antibodies for macrophages. All measurement
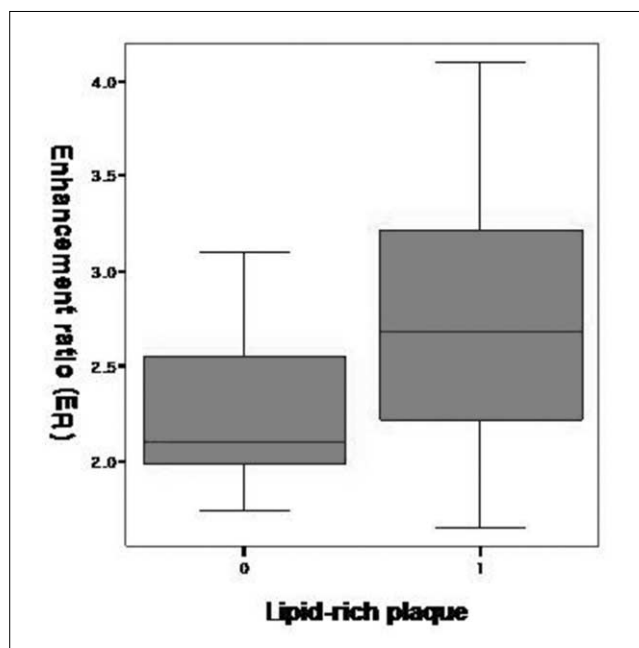

Fig. 2. Box-whisker graph of enhancement ratio of fibrous and lipid-rich quadrants determined by histopathology. Each box describes the distribution of enhancement ratio within one standard deviation.
* Lipid-rich quadrant is labeld as 1 in the x-axis.
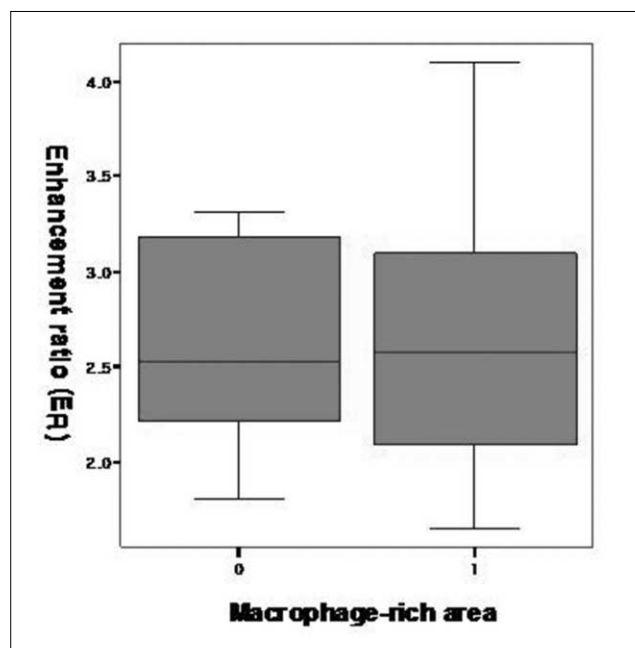* Fibrous quadrant is labeled as 0 in the x-axis.

Fig. 3. Box-whisker graph of enhancement ratio of non macrophage-rich and macrophage-rich quadrants determined by histopathology. Each box describes the distribution of enhancement ratio within one standard deviation.
* Macrophage-rich area is labeld as 1 in the x-axis.
* Non macrophage-rich area is labeled as 0 in the x-axis.

on histological analysis was performed using a computer-assisted quantitative color image analysis system (Image Pro-Plus, Media Cybernetics) in each slices and were expressed in mm^2.

The slices for each rabbit were sequentially numbered to match the image slices between histopathology and MRI. The site and longitudinal extent of plaques were also determined by their distance to the fiduciary points such as side branches or plaque morphology. These were used as references for comparison between MRI and histopathology for each site.

The ER was correlated with the lipid content and macrophage-rich area for each image quadrant.

Statistical Analysis

The statistical significance of differences in ER of plaques according to different plaque types determined by histopathology was assessed using Student's t test for independent samples. Correlations of ER and macrophage-rich areas were performed using Pearson's correlation coefficient. P-values less than 0.05 will be considered statistically significant. SPSS software (Version 10.0; Statistical Package for the Social Sciences, Chicago, IL) was used for statistical evaluation.

Results

Lipid-rich quadrants were 72 and fibrous quadrants were 58. The number of quadrants which had macrophage-rich areas was 105 and that of quadrants which did not have macrophage-rich areas was 25.

The mean area of ROI was 4.2 ± 1.1 mm^2 which varied according to wall thickness. The mean value of maximal wall thickness of each quadrant was 1.1 ± 0.3 mm. ER was significantly higher in lipid-rich quadrants than in fibrous quadrants (mean ER 2.25 ± 0.41 vs. 2.72 ± 0.65, p = 0.013) (Fig. 2). The mean value of macrophage-rich areas was not significantly different between in lipid-rich quadrants and in fibrous quadrants (0.48 ± 0.51 mm^2 vs. 0.58 ± 0.49 mm^2, p = 0.557). ER poorly correlated with macrophage-rich areas when lipid-component was controlled (correlation coefficient −0.203, p = 0.236) (Fig. 3). ER was not different between in the quadrants that had macrophage-rich areas and in the quadrants that did not have macrophage-rich areas (2.57 ± 0.64 vs. 2.63 ± 0.60, p = 0.816).

Discussion

Plaque vulnerability is decided by plaque composition and inflammatory activity rather than the degree of luminal narrowing (1–4). A large lipid-rich necrotic core is a well known factor to reflect plaque vulnerability. Inflammation plays a key role in the whole process of initiation and progression of atherosclerosis and increases vulnerability to rupture as well. Accumulation of macrophages in atherosclerotic plaque is indicative of local inflammatory reaction (13, 14).

MRI is a diagnostic modality for noninvasive imaging of plaque components, such as lipid core, fibrous cap, calcifications, and intraplaque hemorrhage. Because of the limited spatial resolution and low signal-to-noise ratio of MRI, plaque MRI has been studied mainly for carotid artery plaques which have larger size and less motion than coronary artery plaques. Previous studies for carotid atherosclerotic plaques have shown that postcontrast T1-weighted MR images helped to discriminate fibrous cap from necrotic core (6). Fibrous tissue in atherosclerotic plaques was enhanced more than lipid-rich necrotic core and the differences between enhancement of fibrous tissue and lipid-rich necrotic core were significant (5).

Neovessels play a key role in the progression of atherosclerotic plaques by providing routes of leukocyte recruitment into plaque. Several studies reported a higher neovessel count in highly inflamed macrophage-rich atherosclerotic plaques compared to fibrocalcific lesions (8, 9). This suggested that macrophage-rich atherosclerotic plaques, which were active inflammatory plaques, could be enhanced stronger than macrophage-poor atherosclerotic plaques. Kerwin et al. reported that plasma volume and transfer constant correlated with macrophage-rich area using contrast enhanced dynamic MRI in advanced carotid atherosclerotic plaques (7).

The underlying mechanism of plaque enhancement is likely to be mutifactorial and not fully elucidated so far (8, 15, 16). Gadolinium-based agents are known to passively distribute from the intravascular into the extracellular fluid space. Contrast enhancement may be

due to increased permeability, increased extracellular volume, and/or decreased washout of contrast agent (15). Therefore loose matrix, inflammation, and neovascularture were associated with stronger enhancement in atherosclerotic plaque.

In some studies, differentiation of lipid-rich necrotic core from fibrous tissue was potentially possible by using contrast-enhanced MRI (5, 6). Collagen-rich fibrous cap showed moderate enhancement, but the fibrous cap containing neovasculature, inflammatory cell infiltrates or loose matrix showed strong enhancement (6). In our study, however, ER correlated with lipid-rich components. In addition, ER did not correlate with macrophage-rich area, which reflected active inflammation and neovascularization. Lipid-rich area does not necessarily mean avascularity. In our study, necrosis was not a characteristic feature of lipid-rich area in atherosclerotic plaque probably because the plaques were relatively earlier and actively inflammatory stage. Lipid-rich area had loose cellularity which suggested that the lipid-rich plaque had more space for contrast agent to distribute.

In this study, more distributable space was associated with strong enhancement because contrast-enhanced MRI protocol allowed sufficient time for contrast agent molecules to diffuse into lipid-rich areas. In addition, macrophage existed in most quadrants including fibrous quadrant as well as lipid-rich quadrants.

As loose matrix is associated with delayed hyperenhancement using extracellular contrast agents and neovasculature is associated with perfusion parameters, further studies are warranted that account for optimal timing of MRI after contrast administration.

Recently, high resolution wall imaging has been tried in human coronary artery with a 3-T MR unit and a 32-channel receiver coil. Multicontrast plaque imaging and contrast enhanced imaging for evaluation of atherosclerotic plaques in human coronary artery will be possible in near future. This study would be helpful to elucidate the mechanism of contrast enhancement in plaques and to predict vulnerability of plaques based on the association of enhancement and representative components of vulnerabiligy.

Limitation of this study was as follows. We did not analyze neovessels which could be a direct explanation of enhancement. The atherosclerotic plaques in this animal model had abundant lipid-rich area and active inflammation in most quadrants, which resulted in discrepancy of the results between this study and previous studies, where advanced plaque in human carotid artery were used. Interobserver and intraobserver agreement were not obtained. Finally we did not use control to compare enhancement of plaque and normal wall.

Conclusion

Lipid-rich plaques showed stronger enhancement than fibrous plaques using a standard gadolinium-based extracellular contrast agent. Macrophage infiltration did not correlate with degree of enhancement. Further study is warranted that account for optimal time of imaging after contrast injection using various plaque models from early to advanced stages and all possible parameters associated with contrast enhancement.

References

1. Virmani R, Burke AP, Farb A, Kolodgie FD. Pathology of the vulnerable plaque. J Am Coll Cardiol 2006;47:C13-18.
2. Falk E, Shah PK, Fuster V. Coronary plaque disruption. Circulation 1995;92:657-671.
3. Carr S, Farb A, Pearce WH, Virmani R, Yao JS. Atherosclerotic plaque rupture in symptomatic carotid artery stenosis. J Vasc Surg 1996;23:755-566.
4. Virmani R, Kolodgie FD, Burke AP, Farb A, Schwartz SM. Lessons from sudden coronary death: a comprehensive morphological classification scheme for atherosclerotic lesions. Arterioscler Thromb Vasc Biol 2000;20:1262-1275.
5. Yuan C, Kerwin WS, Marina S, et al. Contrast-enhanced high resolution MRI for atherosclerotic carotid artery tissue characterization. J Magn Reson Imaging 2002;15:52-67.
6. Cai J, Hatsukami TS, Ferguson MS, et al. In vivo quantitative measurement of intact fibrous cap and lipid-rich necrotic core size in atherosclerotic carotid plaque; comparison of high-resolution, contrast-enhanced magnetic resonance imaging and histology. Circulation 2005;112:3437-3444.
7. Kerwin WS, O'brien KD, Ferguson MS, Polissar N, Hatsukami TS, Yuan C. Inflammation in carotid atherosclerotic plaque: a dynamic contrast-enhanced MR imaging study. Radiology 2005;241:459-468.
8. Kerwin W, Hooker A, Spilker M, et al. Quantitative magnetic resonance imaging analysis of neovesculature volume in carotid atherosclerotic plaque. Circulation 2003;107:851-856.
9. Calcagno C, Cornily JC, Hyafil F, et al. Detection of neovessels in atherosclerotic plaques of rabbits using dynamic contrast enhanced MRI and 18F-FDG PET. Arterioscler Thromb Vasc Biol 2008;28:1311-1317.
10. Ibrahim T, Makowski MR, Jankauskas A, et al. Serial

contrast-enhanced cardiac magnetic resonance imaging demonstrates regression of hyperenhancement within the coronary artery wall in patients after acute myocardial infarction. J Am Coll Cardiol Img 2009;2:580-588.

11. Lobbes MB, Miserus RJJHM, Heeneman S, et al. Atherosclerosis: contrast-enhanced MR imaging of vessel wall in rabbit model-comparison of gadofosveset and gadopentetate dimeglumine. Radiology 2009;250:682-691.

12. Barkhausen J, Ebert W, Heyer C, Debatin JF, Weinmann HJ. Detection of atherosclerotic plaque with gadofluorine-enhanced magnetic resonance imaging. Circulation 2003;108:605-609.

13. Ohtsuki K, Hayase M, Akashi K, Kopiwoda S, Strauss HW. Detection of monocyte chemoattractant protein-1 receptor

expression in experimental atherosclerotic lesions: an autoradiographic study. Circulation 2001;104:203-208.

14. Ogawa M Ishino S, Mukai T, et al. F-FDG accumulation in atherosclerotic plaques: immunohistochemical and PET imaging study. J Nucl Med 2004;45:1245-1250.

15. Wasserman BA, Smith WI, Trout HH III, Cannon RO III, Balaban RS, Arai AE. Carotid artery atherosclerosis: in vivo morphologic characterization with gadolinium-enhanced double-oblique MR imaging-initial results. Radiology 2002;223:566-573.

16. Aoki S, Aoki K, Ohsawa S, Nakajima H, Kumagai H, Araki T. Dynamic MR imaging of the carotid wall. J Magn Reson Imaging. 1999;9:420-427.

조직병리와 비교한 죽상경화반의 가돌리니움 조영증강 자기공명영상: 토끼 대동맥을 이용한 생체 실험

연세대학교 의과대학 영상의학과, 방사선의과학연구소

최병욱 · 허 진 · 이혜정 · 김영진 · 김태훈 · 최규옥

목적: 죽상경화반 유발 토끼 대동맥에서 자기공명영상을 이용하여 가돌리니움 조영제에 대한 경화반의 조영증강에 어떤 특징이 있는지 알아보고, 경화반 취약성의 대표적인 두 특징인 조직병리학적인 지질풍부 성분과 대식세포 풍부 성분과 비교하여 조영증강이 어떤 조직 소견에서 기인하는지 평가하고자 하였다.

대상 및 방법: 뉴질랜드 흰토끼 (4마리, 무게 3.0 ~ 3.5 kg, 수컷)를 죽상경화반 모델로 사용하였다. 고콜레스테롤 식이와 이중 풍선 손상을 이용하여 대동맥 죽상경화반을 유발하였다. 3-T 자기공명영상을 사용하여 가돌리니움 조영제를 투여하기 전과 후에 T1-강조영상을 얻었다. 자기공명영상과 상응하는 조직병리절편 (n=35)을 4개나 3개의 구역으로 나누었다 (n=130). 자기공명영상에서의 조영증강비 (ER, ER=SIpost/SIpre)를 각 구역마다 계산하여 조직병리의 지질풍부영역과 대식세포 풍부 영역과 비교하였다.

결과: 지질풍부 구역은 72개였고 섬유성구역은 58개였다. 대식세포풍부영역을 포함한 구역은 105개였고 포함하지 않은 구역은 25개였다. 조영증강비는 섬유성구역보다 지질풍부구역에서 높았다 (평균 조영증강비 2.25 ± 0.41 vs. 2.72 ± 0.65, p=0.013). 조영증강비는 지질성분을 제어했을 때 대식세포풍부영역과 잘 비례하지 않았다 (correlation coefficient -0.203, p=0.236).

결론: 표준 가돌리니움 기반의 세포외 조영제를 사용하였을 때 지질풍부 경화반은 섬유성 경화반보다 강한 조영증강을 보였다. 대식세포 침윤은 조영증강 정도와 비례하지 않았다. 초기부터 진행된 병기의 다양한 경화반 모델을 사용하고 조영증강과 관련된 모든 가능한 인자를 사용하여 조영제 투여 후 최적의 영상획득 시간을 결정하는 연구가 필요하다.

통신저자 : 최병욱, (120-752) 서울시 서대문구 신촌동 134, 연세대학교 의과대학 영상의학과 방사선의과학연구소
Tel. 82-2-2228-7400   Fax. 82-2-393-3035   E-mail: bchoi@yuhs.ac